Fabrication of P-, Sb-, and Mg-Doped ZnO Spherical Microcrystals by Laser Ablation in Air

Daisuke Nakamura, Toshinobu Tanaka, Takeshi Ueyama, Tatsuya Ikebuchi, Yuki Fujiwara, Fumiaki Nagasaki, Shuhei Takao, Mitsuhiro Higashihata, Hiroshi Ikenoue and Tatsuo Okada

Graduate School of Information Science and Electrical Engineering, Kyushu University,
744 Motooka, Nishi-ku, Fukuoka 819-0395, Japan
dnakamura@ees.kyushu-u.ac.jp

We have succeeded in growing the ZnO spherical microcrystals by a simple laser ablation in air, and we have obtained ultraviolet (UV) whispering-gallery-mode (WGM) lasing from the sphere under pulsed laser excitation. In this growth technique, a solid ZnO target is rapidly heated by laser-induced plasma, and melted target is splashed from the irradiated spot as droplets. Then, the droplets are crystallized into spherical shapes by the surface tension during the dropping process. This rapid melting and solidifying process may be effective for doping impurities into ZnO. In this study, we fabricated P-, Sb-, and Mg-doped ZnO microspheres, and investigated their structures and optical properties. A blue-shift of UV WGM lasing from Mg-doped ZnO microsphere was obtained, indicating that the band-gap engineering of ZnO microsphere grown by the simple ablation technique was achieved.

1. Introduction

Wide band-gap semiconductor materials have received much attention for their applications in short wavelength photonic devices. Among the materials, zinc oxide (ZnO) has been extensively studied because of its intrinsic properties such as a direct wide band-gap of 3.37 eV and a large exciton binding energy of 60 meV, which is much larger than that of gallium nitride (28 meV) and the thermal energy at room temperature (26 meV). Therefore, ZnO is an excellent candidate material for ultraviolet (UV) emitting devices such as UV light emitting diodes and UV lasers. In addition, ZnO nano/microstructures have attracted considerable attention because of their high crystalline quality and unique structures such as nanowire [1,2], nanowall [3,4], nanorods [5,6], and microdisk [7]. Furthermore, microcavity lasing from these nano/microstructures have been demonstrated [2,4-7]. The lasing action can be classified as random [4,6], Fabry-Perot [2], and whispering-gallery-mode (WGM) [5,7]. In the case of WGM, circular structure such as a sphere or a circular disk is an ideal candidate to achieve much higher light confinement for development of microsized lasers. In our previous study, we have succeeded in synthesizing ZnO spherical microcrystals by a simple atmospheric laser ablation method, and demonstrated UV WGM lasing from the spheres [8,9]. In addition, room-temperature electroluminescence (EL) from the ZnO microsphere/p-GaN heterojunction under forward bias has been observed [10]. In this fabricating method, a solid ZnO target is rapidly heated by laser-induced plasma, and melted target is emitted from the irradiated spot as droplets. Then, the droplets are crystallized into spherical shapes by the surface tension during the dropping process. This rapid melting and solidifying process may be effective for doping impurities into ZnO [11]. In this study, we fabricated doped ZnO spherical crystals using ZnO targets containing dopant, which is Sb, P, or Mg. Sb [12-14] and P [15-17] are candidate acceptors to realize p-type ZnO. On the other hand, Mg-doped ZnO has been investigated for band-gap engineering [18-20]. While most of these researches have been focused on a film structure [21,22], studies on doped ZnO nano/microstructures have been recently increased [23-26]. However, there are few reports on microcavity lasing from the doped ZnO micro/nanostructures [27]. When the acceptor-doping and band-gap engineering of ZnO microspheres are realized by the laser ablation method, electrical pumping and tuning the lasing wavelength can be expected for a ZnO sphere-based microcavity laser. In this paper, we report structural and emission characteristics of doped ZnO microspheres.

2. Experimental and results

2.1 Fabrication of ZnO microspheres

ZnO microspheres were fabricated by a quite simple laser ablation method using a Nd:YAG laser (λ = 1064 nm, 10 Hz) [8,9]. The laser beam was focused on a ZnO sintered target through a focusing lens (f=300 mm) in air with a pulse energy of 30 mJ and the spot size of approximately 200 μm. ZnO sintered targets containing dopant, which is Sb_2O_3, P_2O_5, or MgO were prepared for the growth of doped ZnO microspheres. Droplets produced from the ablation spot of the target surface were crystallized into spherical shapes by the surface tension during the dropping process. The fabricated ZnO microspheres were collected on a proper substrate which was located at approximately 5 mm away from the focal point on the target. A small volume of water was dropped on the substrate before laser ablation in order to increase particle collection efficiency and prevent
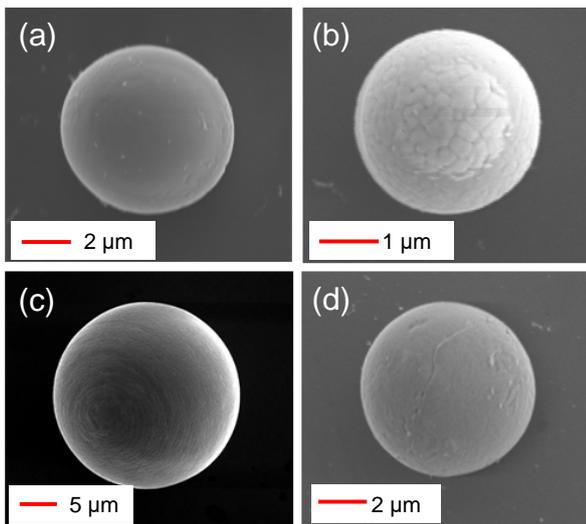
Fig. 1 SEM images of (a) non-doped, (b) P-doped, (c) Sb-doped, and (d) Mg-doped ZnO microspheres. A large number of microspheres with various diameters were synthesized for 2 minutes laser ablation.

coating of the microspheres by undesired nanoparticles, which are simultaneously generated by laser ablation. Figure 1 shows the scanning electron microscope (SEM, KEYENCE VE-7800) images of the ZnO microspheres produced from ZnO target and Sb_2O_3, P_2O_5, and MgO containing targets with 5 wt%. Various sized microspheres with a few micrometers in diameter were successfully fabricated from each target for only 2 minutes laser ablation, and here shows the typical ones. The surface roughness of the doped microspheres was slightly roughened due to incorporation of dopants having different melting points.

## 2.2 Structural characteristics of ZnO microspheres

We have confirmed that the fabricated ZnO microspheres have wurtzite-structured ZnO crystal from the X-ray diffraction [8], and we recently found that one of the
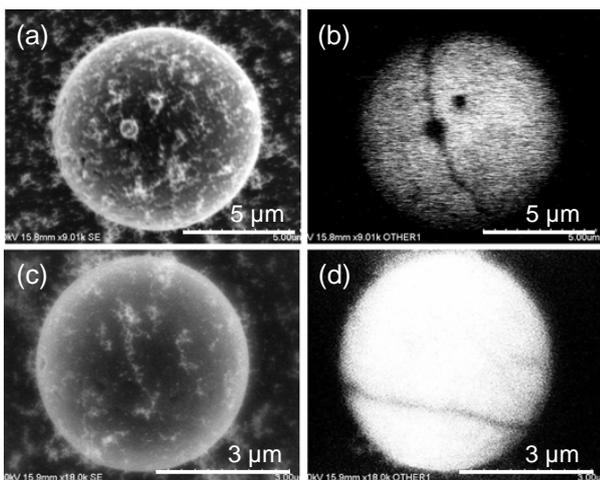
Fig. 2 (a) SEM image and (b) CL image of non-doped ZnO microsphere, and (c) SEM image and (d) CL image of another one. A dark line in the CL images probably shows the crystalline boundary, indicating that the ZnO microspheres consists of polycrystalline structure. The ZnO microspheres are coated by undesired nanoparticles produced during laser ablation.

submicron spheres has a single crystalline structure by transmission electron microscope (TEM) analysis [28]. In this experiment, cathodeluminescence (CL) from ZnO microspheres was measured. Figure 2 (a) and (b) shows the SEM and CL images of a non-doped ZnO microsphere with a diameter of 9.2 µm. The SEM image shows that it had a spherical shape with smooth surface though undesired nanoparticles coated it due to without water. In the CL image, on the other hand, a dark line was observed at the same microsphere. The line probably shows the crystalline boundary, indicating that the ZnO microsphere consists of polycrystalline structure. Similar result was observed from other microsphere as shown in Fig. 2 (c) and (d), hence we conclude that many of microsized ZnO spheres have a poly-crystalline structure and some of submicron spheres consist of a single crystal even though they have spherical shape.

Figure 3 shows the micro-Raman (Horiba, LabRAM ARAMIS) spectra of non-doped and doped ZnO microspheres. These measurements were performed at room temperature. All microspheres showed dominant peaks at 101 and 437 cm^{-1}, which are attributed to the low- and high-E_2 mode of nonpolar optical phonons in the wurtzite structure ZnO [29,30]. In addition, a peak around 238 cm^{-1} was observed only Sb-doped ZnO microspheres. This peak is reported as the local vibrational mode related to Sb in Zn site of the ZnO host lattice [14], indicating Sb atoms were successfully incorporated into the ZnO crystal. According to the first principle calculations, the most stable acceptor complex ($Sb_{Zn}+2V_{Zn}$) is formed in Sb:ZnO system, when Sb occupied Zn antisite (Sb_{Zn}) and is accompanied with two Zn vacancies (V_{Zn}) [31]. For the spectra of P-doped ZnO microsphere, an additional anomalous mode around 478 cm^{-1} emerged, which is a local vibrational mode for the P-O [17]. W.-J. Lee *et al.* reported that a P_{Zn}-$2V_{Zn}$ complex acts as an acceptor [32]. These additional peaks on Raman spectra from Sb- and P-doped ZnO microsphere suggest that the doped microspheres became p-type by the defect complex. The electrical characteristic of the doped microspheres was recently reported [28].
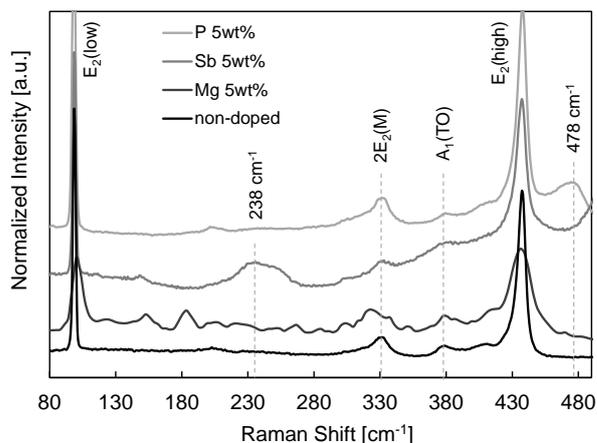
Fig. 3 Raman spectra of non-doped and doped ZnO microspheres. All microspheres have typical ZnO wurtzite structure peaks such as E_2(low) and E_2(high). On the other hand, Sb-doped and P-doped microspheres additionally have 238 cm^{-1} and 478 cm^{-1} peaks, respectively.

Table. 1 Chemical composition of doped ZnO microspheres measured by EDX. The values in round bracket are the standard deviations.

| Containing rate in Target [wt%]		1	2	3	5	10
Concentration of dopant in ZnO microsphere [wt%]	P	1.0 (0.27)	1.2 (0.43)	-	4.1 (1.23)	-
	Sb	1.2 (0.47)	2.3 (0.48)	2.9 (0.40)	4.7 (1.0)	-
	Mg	6.4 (-)	-	-	11.5 (2.6)	16.3 (2.9)
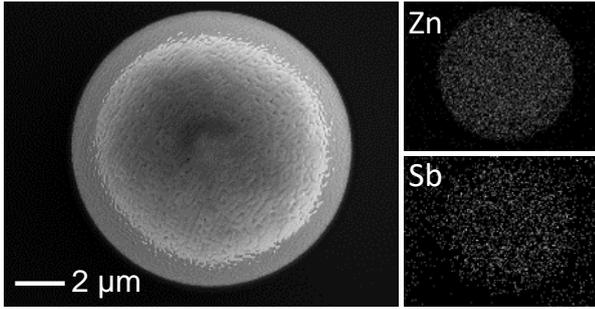
Fig. 4 SEM image of Sb-doped ZnO microsphere and EDX mapping of Zn and Sb elements.

We measured the chemical composition of the doped ZnO microspheres by energy dispersive X-ray spectrometry (EDX). Table 1 shows the average contents in the doped microspheres obtained by measuring three to ten microspheres of various sizes. The values in round bracket are the standard deviations. The dopant contents were roughly corresponded to that of the targets, and the coefficient of variation, (standard deviation)/(average), was about 20 %. The Mg content in microsphere was larger than of the targets. It is attributed to the fact that the vapor pressure of ZnO and Zn is much higher than that of MgO and Mg [18]. Figure 4 shows the SEM image of a Sb-doped microsphere (5 wt%) and EDX mapping of Zn and Sb. The dopant was uniformly distributed, and the concentration of the dopants was independent of the sphere size.

2.3 Emission characteristic of doped ZnO microspheres under pulsed laser excitation

Emission characteristic of doped ZnO microsphere was investigated by a microscopic spectroscopy system [8,9]. The microsphere on the substrate was excited by the third harmonics of a Q-switched Nd:YAG laser (355 nm, 5 ns) and the emission from single microsphere was measured by the spectrometer trough an optical fiber. We have observed UV WGM lasing from non-doped ZnO microsphere, and more recently WGM lasing from Sb- and P-doped ZnO microsphers [28,33]. The lasing threshold of the microspheres was estimated to be 300-650 kW/cm^2, which is relatively higher than that of non-doped one (100 kW/cm^2). This is probably due to decrease of radiative transitions and the roughened surface by doping impurities. On the other hand, Mg-doped ZnO microsphere showed almost the same lasing threshold as non-doped one. Figure 5 shows the emission spectra from the Mg-doped and non-doped ZnO
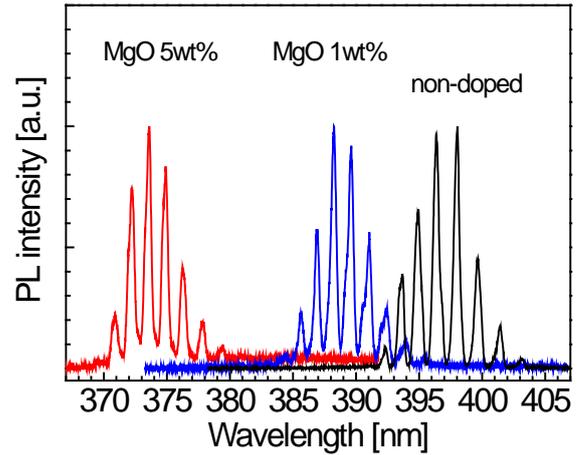
Fig. 5 Emission spectra from non-doped and Mg-doped ZnO microspheres. Further blue shift was observed from that of high Mg content.

microspheres with a diameter of 7.1 μm. Modal peaks in UV region were observed at more than the threshold power density. The mode spacing of the lasing spectra from the microspheres was 1.3 nm, which shows good agreement with the WGM-theoretical mode spacing Δλ [8]. In addition, Mg-doped ZnO microspheres showed a blue-shift compared with non-doped one. The value of the blue-shift
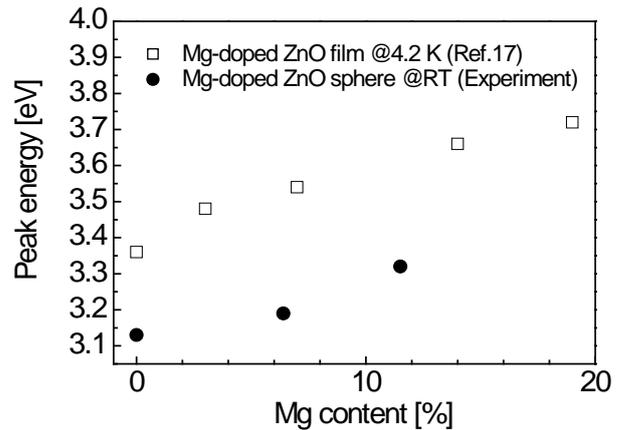
Fig. 6 The maximum peak energy of WGM of Mg-doped ZnO microsphere as a function of Mg content. That of Mg-doped ZnO film (Ref. 18) is shown for comparison.

was increased with increasing Mg concentration. Figure 6 shows the maximum peak energy of the WGM from Mg-doped ZnO microsphere as a function of Mg content. The result of Mg-doped ZnO film [18] is also shown in Fig. 5. The peak energy of WGM was smaller than that of the film. This difference can be attributed to the fact that the WGM lasing is ascribed to the P-band emission [7], which is the exciton-exciton scattering emission of ZnO. The slope of the blue-shift of WGM peak corresponds to that of the luminescence of the Mg doped ZnO film, indicating that the band-gap engineering of ZnO microsphere is achieved. In other word, lasing wavelength of ZnO microsphere can be tuned by Mg concentration. However, no lasing behavior was observed from microspheres fabricated from a target containing MgO 10 wt% due to low UV emission intensity.

Basically, the stoichiometry control of doped ZnO film using laser ablation is realized by preparation of different composition targets and fabrication under optimized growth conditions such as substrate temperature, gas pressure and laser intensity [18]. On the other hand, one laser intensity condition was performed in the present study. The laser ablation conditions such as laser intensity and laser spot size will affect heating temperature and heating rate of the target, which may influence the doping behavior such as dopant concentration. Thus, a further investigation of the dependence of different laser conditions will be essential in the stoichiometry control of doped ZnO microspheres.

3. Conclusion

We succeeded in fabricating doped ZnO microspheres by the simple atmospheric ablation method. It was confirmed that the fabricated microspheres had wurtzite structure and contained the dopant by micro-Raman and energy dispersive X-ray spectrometry analysis. The each dopant content was corresponded to that of the targets. The additional Raman peaks from Sb- and P-doped ZnO microsphere suggested that acceptor complexes ($Sb_{Zn}+2V_{Zn}$ and $P_{Zn}-2V_{Zn}$) were formed in ZnO crystal. The ultraviolet whispering-gallery-mode lasing action was observed from doped ZnO microsphere because of high light-confinement property resulted from the spherical microcavity effect. Experimental results were in good agreement with WGM theory in terms of mode spacing. Furthermore, a blue-shift was observed from the Mg-doped ZnO microsphere, and the value of blue-shift could be tuned by changing Mg concentration.

References

[1] Y. Li, G. W. Meng, L. D. Zhang and F. Phillipp: Appl. Phys. Lett., 76 (2000) 2011.
[2] M. H. Huang, S. Mao, H. Feick, H. Yan, Y. Wu, H. Kind, E. Weber, R. Russo and P. Yang: Science, 292, (2001) 1897.
[3] J. Y. Lao, J. Y. Huang, D. Z. Wang, Z. F. Ren, D. Steeves, B. Kimball and W. Porter: Appl. Phys. A, 78, (2004) 539.
[4] K. Harada, S. Nakao, M. Takahashi, M. Higashihata, H. Ikenoue, D. Nakamura, Y. Nakata and T. Okada: Appl. Phys. B, 119, (2015) 469.
[5] J. Dai, C. X. Xu, K. Zheng, C. G. Lv and Y. P. Cui: Appl. Phys. Lett., 95, (2009) 241110.
[6] S. F. Yu, C. Yuen, S. P. Lau, W. I. Park and G.-C. Yi: Appl. Phys. Lett., 84, (2004) 3241.
[7] R. Chen, B. Ling, X. W. Sun and H. D. Sun: Adv. Mater., 23, (2011) 2199.
[8] K. Okazaki, T. Shimogaki, K. Fusazaki, M. Higashihata, D. Nakamura, N. Koshizaki and T. Okada: Appl. Phys. Lett., 101, (2012) 211105.
[9] D. Nakamura, T. Shimogaki, K. Okazaki, M. Higashihata, H. Ikenoue and T. Okada: J. Laser Micro/Nanoeng., 8, (2013) 296.
[10] N. Tetsuyama, K. Fusazaki, Y. Mizokami, T. Shimogaki, M. Higashihata, D. Nakamura and T. Okada: Opt. Exp., 22, (2014) 10026.
[11] A. Tsukazaki, A. Ohtomo, T. Onuma, M. Ohtani, T. Makino, M. Sumiya, K. Ohtani, S. F. Chichibu, S. Fuke, Y. Segawa, H. Ohno, H. Koinuma and M. Kawasaki: Nat. Mater., 4, (2004) 42.
[12] J. Z. Zhao, H. W. Liang, J. C. Sun, J. M. Bian, Q. J. Feng, L. Z. Hu, H. Q. Zhang, X. P. Liang, Y. M. Luo and G. T. Du: J. Phys. D Appl. Phys., 41, (2008) 195110.
[13] F. X. Xiu, Z. Yang, L. J. Mandalapu, D. T. Zhao and J. L. Liu: Appl. Phys. Lett., 87, (2005) 252102.
[14] K. Samanta, P. Bhattacharya, and R. S. Katiyar: J. Appl. Phys., 108, (2010) 113501.
[15] J.-H. Lim, C.-K. Kang, K.-K. Kim, I.-K. Park, D.-K. Hwang and S.-J. Park: Adv. Mater., 18, (2006) 2720.
[16] X. Fang, J. Li, D. Zhao, D. Shen, B. Li and X. Wang: J. Phys. Chem. C, 113, (2009) 21208.
[17] J. D.Ye, S. L. Gu, S. M. Zhu, S. M. Liu, Y. D. Zheng, R. Zhang, Y. Shi, Q. Chen, H. Q. Yu and Y. D. Ye: Appl. Phys. Lett., 88, (2006) 101905.
[18] A. Ohtomo, M. Kawasaki, T. Koida, K. Masubuchi, H. Koinuma, Y. Sakurai, Y. Yoshida, T. Yasuda and Y. Segawa: Appl. Phys. Lett., 72 (1998) 2466.
[19] Y. S. Wang, P. T. Thomas and P. O'Brien: J. Phys. Chem. B, 110, (2006) 21412.
[20] F. K. Shan, G. X. Liu, W. J. Lee and B. C. Shin: J. Cryst. Growth, 291, (2006) 328.
[21] T. H. Kim, J. J. Park, S. H. Nam, H. S. Park, N. R. Cheong, J. K. Song and S. M. Park: Appl. Sur. Sci., 255, (2009) 5264.
[22] F. K. Shan, B. I. Kim, G. X. Liu, Z. F. Liu, J. Y. Sohn, W. J. Lee, B. C. Shin and Y. S. Yu: J. Appl. Phys., 95, (2004) 4772.
[23] C.-H. Ku, H.-H. Chiang and J.-J. Wu: Chem. Phys. Lett., 404, (2005) 132.
[24] P. Shimpi, Y. Ding, E. Suarez, J. Ayers and P.-X. Gao: Appl. Phys. Lett., 97, (2010) 103104.
[25] S. S. Lin, J. I. Hong, J. H. Song, Y. Zhu, H. P. He, Z. Xu, Y. G. Wei, Y. Ding, R. L. Snyder and Z. L. Wang: Nano Lett., 9, (2009) 3877.
[26] H. Tang, B. J. Kwon and J.-Y. Park: Phys. Status Solidi A, 207, (2010) 2478.
[27] S. Kalusniak, S. Sadofev, J. Puls and F. Henneberger: Laser & Photon. Rev., 3, (2009) 233.
[28] F. Nagasaki, T. Shimogaki, T. Tanaka, T. Ikebuchi, T. Ueyama, Y. Fujiwara, M. Higashihata, D. Nakamura and T. Okada: Jpn. J. Appl. Phys., 55, (2016) 08RE07.
[29] J. M. Calleja and M. Cardona: Phys. Rev. B, 16, (1977) 3753.
[30] C. Gray, J. Cullen, C. Byrne, G. Hughes, I. Buyanova, W. Chen, M. O. Henry and E. McGlynn: J. Cryst. Growth, 429, (2015) 6.
[31] S. Limpijumnong, S. B. Zhang, S. H.Wei and C. H. Park: Phys. Rev. Lett., 92, (2004) 155504.
[32] W.-J. Lee, J. Kang and K. J. Chang: Phys. Rev. B, 73, (2006) 024117.
[33] Y. Fujiwara, T. Ikebuchi, T. Ueyama, T. Tanaka, F. Nagasaki, M. Higashihata, D. Nakamura and T. Okada: Proc. SPIE, 9749, (2016) 97490T.